Effects of truncated Gaussian beam on the performance of fiber optical synthetic aperture system*

LIU Li(刘丽)**, **WANG Chang-wei**(王长伟), **and JIANG Yue-song**(江月松)
School of Electronic and Information Engineering, Beijing University of Aeronautics and Astronautics, Beijing 100191, China

(Revised 28 December 2011)

In the fiber optical synthetic aperture (FOSA) system, the diffraction of the Gaussian beam limited by the aperture in exit pupil plane of fiber collimator is studied theoretically, and the axial and transverse irradiance distributions are obtained. The point spread function (PSF) and modulation transfer function (MTF) of the truncated Gaussian beam array are computed numerically with different truncation factors. The results show that the diffraction of the truncated Gaussian beam array agrees with the uniform-beam Rayleigh diffraction when the truncation factor is less than 0.5, but little power is transmitted. The PSF and MTF are degraded, but more power can be contained when the truncation factor is larger. The selection of the truncation factor is a trade-off between the loss of transmission and the qualities of PSF and MTF in practical application.

Document code: A **Article ID:** 1673-1905(2012)03-0216-4
DOI 10.1007/s11801-012-9227-2

The optical synthetic aperture (OSA) system, which uses an array of independent sub-apertures to realize imaging of a large aperture system, has become an effective technique to achieve high angular resolution[1]. The key aspects of the design of the OSA system have been under investigation in many developed countries[2,3]. In recent years, several universities and research institutions in China have began to concentrate on theoretical researches of imaging principles and array configuration, etc[4,5]. Clearly, as the number of sub-apertures increases, beam transportation, optical path compensation and beam combination in the OSA system become more complex and difficult to built. To reduce the complexity, Froehly and Connes[6] proposed an alternative solution to use optical fibers in the interferometer. Many researchers have been working on the applications of fiber in radio, optical and millimeter interferometers[7,8]. Some interferometers using fibers have been realized or are under construction for beam combination and beam transportation. Optical fibers can be used in both space- and ground-based systems. Thanks to the flexibility and portability of optical fibers, the systems can be smaller, lighter and more integrated and compact than conventional ones, leading to reduced difficulties of payload and launch, which is especially attractive for a space-based system.

However, some new problems with the use of optical fibers can be introduced. For example, the fundamental-mode field distribution for a single-mode (SM) fiber is nearly a Gaussian function, but not a uniform function, which is different from that of the conventional optical systems and can inevitably affect the OSA imaging systems. But few people research this effect in detail. In this paper, we just focus on how the property of the fiber transforming the uniform field into a Gaussian field influences the OSA imaging performance, which is mainly based on the point spread function (PSF) and modulation transfer function (MTF). It must be assumed that the atmospheric turbulence error can be neglected, sub-aperture systems are performed in perfect case, and the fibers do not introduce any noise or wavefront error. The fiber optical synthetic aperture (FOSA) imaging system used in this paper is shown in Fig.1. The SM fibers carry the beams from each telescope to the combination sub-system, where a lenslet or microlens array is used to collimate the fiber outputs and arrange the fibers to an array for coherently forming a phased image on the detector. There are only three sub-telescopes shown in Fig.1 for simplification.

* This work has been supported by the National High Technology Research and Development Program of China (No.2007AA12Z114).
** E-mail:catty118 @ee.buaa.edu.cn

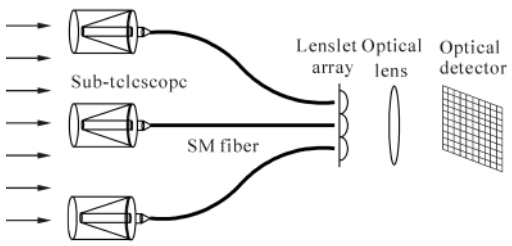

Fig.1 Schematic diagram of the FOSA system

The fundamental-mode field distribution for an SM fiber in transverse plane is approximated by a Gaussian function[9] as follows,

$$u = u_0 \frac{\omega_0}{\omega(z)} \exp\left[-\frac{r_0^2}{\omega^2(z)} \right], \tag{1}$$

where r_0 is the radial coordinate, ω_0 is the waist radius, and $\omega(z)$ is the radius corresponding to the radial distance.

In the FOSA system, the output of each fiber is collimated by a microlens, so each Gaussian beam is collimated and truncated by the collimation lens with a limited diameter. For an ideal collimation system, the waist of the Gaussian beam is at the front focal plane. Providing that the collimation lens is an aberration-free spherical lens with focal length of f and the radius of a, we define the truncation factor as the ratio of $F=a/\omega(f)$. Therefore, the truncation Gaussian (TG) intensity distribution after a sub-pupil is

$$I(r_0) = I_0 \left(\frac{\omega_0}{a} F \right)^2 \exp\left[-2F^2 \frac{r_0^2}{a^2} \right], \ r_0 \le a \ . \tag{2}$$

The power transmitted by the truncated beam is

$$P = 2\pi \int_0^a I r_0 \, \mathrm{d}\, r_0 = \frac{\pi I_0 \omega_0^2}{2} \left[1 - \exp(-2F^2) \right] . \tag{3}$$

Therefore, the power transmission ratio is

$$\eta = \frac{P}{2\pi \int_0^{+\infty} I(r_0) r_0 \, \mathrm{d}\, r_0} = 1 - \exp(-2F^2) . \tag{4}$$

The Gaussian beams shaped by the collimators are focused by the Fourier lens with focal length of f'. According to Fraunhofer diffraction theory, assuming that the wavefront phases of beams from all fibers have no random fluctuation, the intensity distribution on the image plane is given by

$$I(r) = I_0 \left(\frac{k\omega_0 F}{f'a} \right)^2 \left| \int_0^a \exp\left[-F^2 \frac{r_0^2}{a^2} \right] J_0\left(\frac{krr_0}{f'} \right) r_0 \, \mathrm{d}\, r_0 \right|^2 , \tag{5}$$

where J_0 is the zero-order Bessel function of the first kind, r_0 and r denote radial coordinates in the pupil plane and in the image plane, respectively.

We consider the system with N sub-telescopes, assuming that all sub-waves have identical phase, so the PSF in the image plane is

$$I_{\text{array}}(r) = I(r) \times \left| \sum_{n=1}^{N} \exp\left(-\mathrm{i} \frac{k}{f'} r r_n \right) \right|^2 , \tag{6}$$

where r_n denotes the position of the nth sub-pupil in the exit pupil plane. For convenience, the normalized intensity distributions (i.e.,PSF)[10] are derived for both uniform parallel beam and TG beam as

$$I'_{\text{u}}(r') = \left[\frac{2J_1(\pi r')}{\pi r'} \right]^2 \times \left| \sum_{n=1}^{N} \exp(-\mathrm{i}\pi r' r'_n) \right|^2 , \tag{7}$$

$$I'_{\text{g}}(r') = \frac{8F^2}{1 - \mathrm{e}^{-2F^2}} \left| \int_0^1 \exp\left[-F^2 r_0'^2 \right] J_0(\pi r' r'_0) r'_0 \, \mathrm{d}\, r'_0 \right|^2 \times \left| \sum_{n=1}^{N} \exp(-\mathrm{i}\pi r' r'_n) \right|^2 , \tag{8}$$

where $r'_0 = r_0 / a$, $r' = 2ar / \lambda f$, and $I' = P\pi a^2 / (N\lambda f)^2$.

To describe the influence of the Gaussian intensity distribution in the optical fibers on the PSF and MTF, several numerical simulations are done. Fig.2 presents the normalized on-axis intensity (i.e., $I'(0)$) for various F. The maximum intensity decreases as the truncation factor grows, and it can achieve 92.4% when F = 1. However, power transmission is very low when the truncation factor is larger, which is shown in Fig.3.

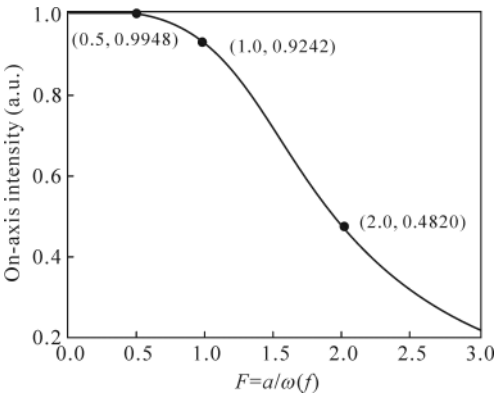

Fig.2 On-axis intensity as a function of *F*

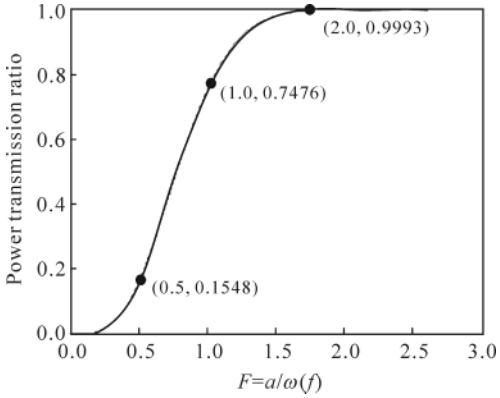

Fig.3 Power transmission as a function of *F*

We take a four-sub-aperture array for example, which is shown in Fig.4(a), and the 3D and 2D PSFs for different truncation factors are illustrated in Fig.4(b), (c) and (d), where x and y denote the axes in the rectangular coordinate system corresponding to r' in the radial coordinate system. It is obvious that the central lobe of PSF becomes smaller and the number of side lobes trends to increase as F increases. The PSF of the TG beam is the same as that of the uniform parallel beam when $F = 0.5$. While $F = 1$, the on-axis intensity of the TG is smaller, and the side lobes increase both in width and in height. When $F = 2$, the side lobe effect is so serious that the central lobe is nearly overwhelmed by side lobes, and the energy contained in the central lobe is smaller. This is due to the diffraction of the TG beam contains the diffractions of the circular aperture and the Gaussian beam. When the truncation factor is small, the former is dominant, and then the diffraction of the TG beam can be replaced by the circular aperture diffraction of the uniform parallel beam. With the increase of the truncation factor, the effect of circular aperture trends to smaller, while the diffraction of the Gaussian beam becomes more important gradually.

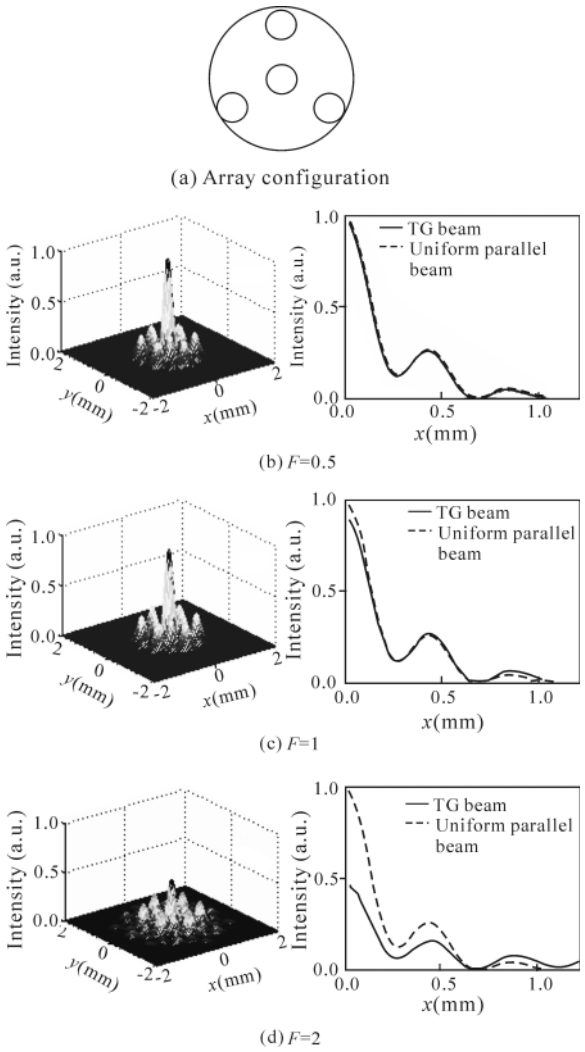

Fig.4 Four-sub-aperture array configuration and PSFs for different truncation factors

It is shown that the cut-off frequency in the MTF decreases as truncation factor increases in Fig.5. Besides that, there are more fluctuations in the middle frequency region, and even zero values appear within the cut-off frequency, which means the loss of the corresponding spatial frequency information.

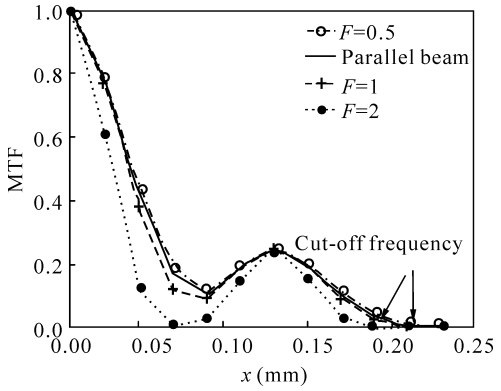

Fig.5 MTF curves for different truncation factors

We analyze the Gaussian properties of fiber array in the FOSA system theoretically, and the effects of the truncated Gaussian beam on the PSF and MTF in the image plane are simulated numerically. The results show that the diffraction of TG beams nearly agrees with that of uniform parallel beams when the truncation factor is smaller than 0.5. As the truncation factor increases, the side lobes of PSF grow, the central lobe decreases, and the middle frequency region of MTF fluctuates greatly, which leads to worse image quality. However, when the truncation factor is smaller than 0.5, the energy transmitted by the truncated beam remains just 16%. In consideration of coupling efficiency, the rest power is very little. Therefore, it is advised that the truncation factor should be around 1 in practical applications.

References

[1] WU Feng, WU Quanying and QIAN Lin, Appl. Opt. **48**, 643 (2009).

[2] B. J. Daniel, M. R. Bolcar, J. R. Schott and J. R. Fienup, Proc. SPIE **6958**, 69580K-1 (2008).

[3] A. J. Stokes, B. D. Duncan and M. P. Dierking, Proc. SPIE **7323**, 73230M-1 (2009).

[4] HAN Ji, WANG Dayong and LIU Hancheng, Journal of Optoelectronics • Laser **18**, 649 (2007). (in Chinese)

[5] WANG Chang-wei, JIANG Yue-song, LIU Li and WANG Hai-yang, Journal of Optoelectronics • Laser **21**, 424 (2010). (in Chinese)

[6] P. Connes, C. Froehly and P. Facq, Colloquium on Kilometric Optical Arrays in Space, Proc. ESA, 49 (1984).

[7] I. Biswas, C. A. Schuetz, R. D. Martin, M. S. Mirotznzk, S. Shi, G. J. Schneider, J. Murakowski and D. W. Prather, Proc. SPIE **6739**, 67390P-1 (2007).

[8] L. Delage, F. Reynaud and A. Lannes, Appl. Opt. **39**, 6406 (2000).

[9] SONG Feijun, YANG Guoguang and YU Jinzhong, Information Photonics Physics, Beijing: Peking University Press, 293 (2006).

[10] Virendra N. Mahajan, J. Opt. Soc. Am. A **3**, 470 (1986).